Bioscience, Biotechnology, and Biochemistry, 2021, Vol. 85, No. 2, 340-350

doi: 10.1093/bbb/zbaa013
Advance access publication date: 20 January 2021
REGULAR PAPER

REGULAR PAPER

Generation and characterization of monoclonal antibodies against mature hepcidin and its application to neutralization and quantitative alteration assay

Shinji Sakamoto [1,*] Mika Kirinashizawa,[1] Yumi Mohara,[1] and Yoshihiro Watanabe[1,†]

[1]Pharmaceutical Frontier Research Laboratories, Japan Tobacco Inc., Yokohama City, Japan

*Correspondence: Shinji Sakamoto, shinji.sakamoto@jt.com
†Present address: Yoshihiro Watanabe, Innovative Clinical Research Center, Kanazawa University Hospital, Kanazawa, Japan.

ABSTRACT

Hepcidin regulates the quantity of ferroportin (FPN) on cellular membrane. In our cell assay expressing ferroportin labeled with green fluorescence, FPN was internalized and degraded only after treatment with hepcidin-25, not hepcidin-22 or hepcidin-20, leading to accumulation of cellular iron. Thus we generated murine monoclonal antibodies (mAbs) against hepcidin-25, and then characterized and validated their functions. Among them, several mAbs showed a neutralizing activity that may prevent ferroportin internalization induced by hepcidin-25. To measure hepcidin level in various fluids, mAbs specific for human and rat hepcidin-25 were selected. As for rat, a sandwich ELISA developed using clone rHN1 as capture antibody and biotinylated clone mHW1 as a detection reagent had high sensitivity, allowing for the detection of 1-100 ng/mL of hepcidin-25. Rat hepcidin-25 level in plasma was measured at an average concentration of 63.0 ng/mL in healthy condition, and at 218.2 ng/mL after stimulation of lipopolysaccharide.

Graphical Abstract

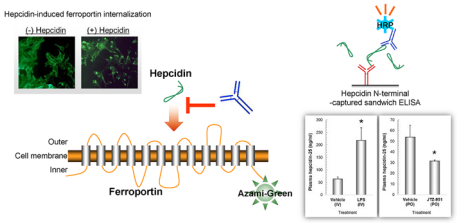

Characterization of hepcidin monoclonal antibodies and its application for suppressing ferroportin degradation and detecting quantitative alteration.

Keywords: hepcidin, ferroportin, monoclonal antibody, neutralization, rodent

Received: 5 August 2020; **Accepted:** 15 September 2020

Iron is an essential element for all living organisms; however, it also produces toxic oxidants. Thus iron homeostasis is strictly regulated in mammals. Hepcidin, which is initially found as an antimicrobial peptide in human urine and serum, well regulates iron metabolism (Krause *et al.* 2000; Park *et al.* 2001; Atanasiu *et al.* 2007), that is, binding of hepcidin to its receptor ferroportin (FPN) suppresses intestinal iron absorption and iron efflux from hepatocytes and macrophages, while decreased hepcidin level enhances iron absorption and efflux (Nemeth *et al.* 2004). Therefore, hepcidin is thought to be deeply involved in many pathologies such as anemia following decrease of iron availability. Anemia is a common and important issues associated with chronic kidney disease (CKD), which is caused by erythropoietin deficiency, iron-restricted erythropoiesis, inflammation, hypoxia, and vitamin D deficiency. Anemia further causes poor quality of life, progression of CKD, increased risk of cardiovascular events, and mortality. Recent evidences, besides its role in anemia, suggest that hepcidin plays a role in the pathogenesis and progression of kidney injury via modulation of iron-mediated oxidant injury. Monitoring hepcidin level is believed to be helpful for the management of chronic diseases, because hepcidin could be predictive of iron status and the response to iron supplementation or erythropoietin-stimulating agents (Wang and Babitt 2016; Ueda and Takasawa 2017; Ginzburg 2019). However, despite development of various hepcidin assays and accumulation of experimental data measured by various methods that enable their comparison, insight and information about clinical significance of hepcidin-25 in treatment for anemia and kidney injury in patients seems to be still scarce (Butterfield *et al.* 2010; Konz *et al.* 2014; Dahlfors *et al.* 2015; Lefebvre *et al.* 2015; Girelli *et al.* 2016; Abbas *et al.* 2018). Furthermore, several recent studies deal with the implication of hepcidin to metabolic disease characterized by pathogenesis that increase the risk for cardiovascular disease and diabetes, such as abdominal obesity, dyslipidemia, and hypertension. In nonalcoholic fatty liver disease (NAFLD) patients, an inadequate hepcidin production was observed compared to controls, although not as low as in hereditary hemochromatosis (Barisani *et al.* 2008). In contrast, Senates *et al.* found that hepcidin levels are elevated in NAFLD, and serum hepcidin could be associated with cholesterol and triglycerides levels, but not with iron parameters (Senates *et al.* 2011). This was not consistent with other finding that serum hepcidin and HAMP (hepcidin antimicrobial peptide) mRNA in liver correlate to body iron content but not to the degree of steatohepatitis or lipid status (Marmur *et al.* 2018). Whereas in obese patients, hepcidin expression was increased and negatively correlated with declined levels of adiponectin mRNA (Pihan-Le Bars *et al.* 2016). Obesity was associated with increased levels of proinflammatory cytokines such as IL-6 and TNF-α (Jr *et al.* 2010). The expression of hepcidin was increased in adipocytes in response to inflammatory stimuli, including IL-6 or lipopolysaccharide (LPS) (Hintze and McClung 2011). Additionally, adipose tissue can release IL-6 and TNF-α, which enhance hepcidin expression (Andrade-Oliveira *et al.* 2015). Although the precise mechanism of obesity-associated up-regulation of hepcidin remains elusive, adipose tissue is an additional source of hepcidin and seems to be not a little involved in pathogenesis and progression of metabolic diseases (Ueda and Takasawa 2017).

Hepcidin is produced as a pre–prohormone (84 amino acids) containing a typical N-terminal 24 amino acid endoplasmic reticulum-targeting signal sequence firstly in mainly in liver, and then prohormone (60 amino acids) is processed to hormone (25 amino acids). The posttranslational processing of prohepcidin to hepcidin is mediated by the prohormone convertase furin (Valore and Ganz 2008; Gagliardo *et al.* 2009). On the other hand, 20 and 22 amino acid metabolites of hepcidin exist in the urine. This conversion may be regulated by alpha-1 antitrypsin (Pandur *et al.* 2009; Kroot *et al.* 2011). Hepcidin-25 is a tightly folded polypeptide with 32% beta sheet character and a hairpin structure stabilized by 4 disulfide bonds (Hunter *et al.* 2002). Additionally, N-terminal amino acids of hepcidin-25 are known to be important for its function (Nemeth *et al.* 2006; Clark *et al.* 2011).

Hence, we focused on hepcidin and its receptor FPN axis, and tried to develop analytical tools, including a cell-based assay, to evaluate the biological activity of hepcidin. To this end, we also produced a panel of murine monoclonal antibodies (mAbs) against hepcidin. Regarding strategy for generating mAbs specific for hepcidin-25, we used N-terminal amino acid sequences that exist only in hepcidin-25, and but not in hepcidin-22 or hepcidin-20, as an antigen. In addition to a validation of neutralizing activity of each mAbs generated, a sandwich ELISA was also developed as an easy quantitative and reproducible method to monitor the level of hepcidin-25 fluctuating with the treatment of inflammatory stimuli or suppressor in rodent models.

Materials and methods

Hepcidin synthesis

All synthetic forms of hepcidin (hepcidin-25, hepcidin-22, and 20 amino acid forms) were obtained from the Peptide Institute, Inc. (Osaka, Japan), where their structures were precisely examined, that is, to determine whether each hepcidin form had proper conformational structure, including 4 disulfide bonds to stabilize its hairpin structure.

Generation of mAbs against hepcidin

This animal study was conducted in accordance with the Japanese Law for the Humane Treatment and Management of Animals (Law No. 105, October 1, 1973). Prior to the animal study initiation, the outline of animal study protocol had been reviewed by the Institutional Animal Care and Use Committee of the Central Pharmaceutical Research Institute, Japan Tobacco, Inc. To generate mAbs against hepcidin-25, 5-week-old male ICR mice (Charles River Laboratories, Inc., Yokohama, Japan) were immunized with human, rat, and mouse hepcidin (25 amino acids). To generate mAbs against N-terminal sequence of hepcidin-25, 5-week-old male ICR mice (Charles River Laboratories, Inc.) were immunized with a peptide DT**H**FPISGSGSG for human, or DT**N**FPISGSGSG for rat and mouse, both of which were synthesized by Scrum, Inc. (Tokyo, Japan). These peptide conjugated to ovalbumin (OVA; Thermo Fisher Scientific K.K., Tokyo, Japan) were injected into mouse foot-pad for immunization 4-5 times at weekly intervals. Saponin (FUJIFILM Wako Pure Chemical Corporation, Kyoto, Japan) was used as an adjuvant only for the first immunization. Popliteal lymph node cells were fused with a mouse myeloma cell line, PAI, using PEG4000 (Roche Diagnostics GmbH, Mannheim, Germany) (Sakamoto *et al.* 2001). Supernatants of the growing hybridomas were tested by ELISA with each antigen and negative control peptides.

ELISA for analysis of mAbs specificity

ELISA was performed at room temperature. Briefly, the wells of 96-well streptavidin-coated plate (Nalge Nunc International Corporation, Rochester, NY) were incubated for 1 h with 2 µg

biotinylated peptide in 50 µL phosphate-buffered saline (PBS). The wells were then blocked for 2 h with Blocking One (Nacalai Tesque, Inc., Kyoto, Japan). After washing with PBS-Tween 20 (PBS/T; Medicago, Inc., Uppsala, Sweden), the wells were incubated for 1 h with 5 µg/mL mAbs in 50 µL PBS/T. The wells were subsequently washed 3 times with PBS/T and incubated for 1 h with 50 µL horseradish peroxidase (HRP)-labeled antimouse IgG antibody (GE Healthcare, Chicago, IL) in PBS/T containing 0.5% Blocking One (Nacalai Tesque, Inc.). After washing 4 times with PBS/T, the wells were incubated with 100 µL tetramethyl bendidine (TMB; Bio-Rad Laboratories, Inc., Hercules, CA). The reaction was terminated by 25 µL 0.5N sulfuric acid, and the absorbance at 450 nm was read on a microplate reader, SoftMax Pro (Molecular Devices, LLC, Sunnyvale, CA). Antigen-coated direct ELISA mode was also occasionally used for analysis of mAb specificity. To analyze the capability of antigen capture of mAbs, the wells of a protein G–coated plate (Nalge Nunc International Corporation) were incubated for 1 h with 0.25 µg mAbs in 50 µL PBS. After blocking, the wells were incubated for 1 h with 2 µg/mL biotinylated peptide in 50 µL PBS/T. The captured peptide was then detected by HRP-labeled streptavidin (GE Healthcare). If necessary, reagents such as peptide, antibody, and synthetic hepcidin were biotinylated by EZ-Link NHS-PEG4-Biotin (Thermo Fisher Scientific K.K.) in accordance with the manufacturer's instructions.

Establishment of FPN with green fluorescence protein tag expressing cell line

We established T-REx 293 cell line expressing human FPN with a C-terminal green fluorescent protein, Azami-Green (AG; MBL Co., Ltd., Aichi, Japan), under the control of tetracycline-inducible CMV promoter. Briefly, a cDNA for human FPN was cloned into the phmAG-MNL vector (MBL Co., Ltd.). The plasmid was digested to obtain the FPN-AG construct. A pcDNA4/TO vector (Invitrogen, Carlsbad, CA) was digested and ligated with the FPN-AG insert, in accordance with the manufacturer's directions. The ligation was transfected into JM109 *Escherichia coli* and ampicillin-resistant colonies were selected. Plasmids were purified (Qiagen, Valencia, CA) and sequenced. T-REx 293 cells (Invitrogen) were grown in D-MEM with 10% Tet System Approved fetal bovine serum (Tet-free FBS; Clontech Laboratories, Inc., Mountain View, CA) containing penicillin (61.5 mg/mL), streptomycin (0.1 mg/mL), and blasticidin (0.1%). Cells were transfected with 0.2 µg DNA using Gene Jammer Reagent (Stratagene, San Diego, CA) as per the manufacturer's protocol. After transfection, the cells were placed into selective medium containing zeocin (400 µg/mL) and blasticidin (0.1%). After 2-3 weeks, stably transfected colonies that showed induction of FPN-AG in response to 1 µg/mL tetracycline (Tet; Invitrogen) were selected. Transfected cells were incubated at 37 °°C in 5% CO_2.

FPN internalization/degradation assay and ferritin measurement

Briefly, T-REx 293 FPN-AG cells were plated in Optilux 96-well poly-D-lysine-coated plates (Becton, Dickinson and Company, Tokyo, Japan) at 20 000 cells/well and induced overnight with final 1 µg/mL Tet at 37°C. Induction medium was replaced with assay medium (D-MEM with 10% Tet-free FBS) containing hepcidin. Cells were incubated at 37°C at varying concentrations of hepcidin for varying amounts of times (generally 4-8 h). FPN internalization was estimated by cell surface expression of FPN-AG visualized with cellular imaging. Uninduced (non-FPN-AG expressing) cells served as a negative control. Images were captured using an ArrayScan VTI HCS reader (Thermo Fisher Scientific K.K.) equipped with Zeiss microscope optics and Hamamatsu ORCA-ER CCD camera. FPN degradation was quantified in terms of fluorescence intensity unit (FIU) at 460/505 nm, as detected signal derived from FPN-AG, measured by fluorescence plate reader (Tecan Trading AG, Männedorf, Switzerland).

Regarding ferritin measurement, cells were plated at 20 000 cells/well overnight, incubated with 20 µM FAC for 24 h, and then induced with 0.1 µg/mL Tet in the presence or absence of hepcidin-25 for 24 h again. After harvesting cells, cellular lysate was used for both ferritin measurement and protein quantitative assay. Ferritin levels were determined using an AssayMax Human Ferritin ELISA Kit (Assaypro LLC, St. Charles, MO) in accordance with the manufacturer's instructions and were normalized for the total protein concentration in each sample, as determined by the BCA assay (Pierce Biotechnology, Inc., Rockford, IL).

FPN degradation assay for analysis of mAbs neutralizing activity

T-REx 293 FPN-AG cells were plated in Optilux 96-well poly-D-lysine-coated plates (Becton, Dickinson and Company) at 20 000 cell/well and induced overnight as described above. Prior to treating cells, mAbs were mixed with hepcidin-25 at concentrations indicated in Figure 5, and incubated for 1 h at room temperature. After treating cells with mAbs–hepcidin mixture for 4-8 h, fluorescence intensity signal derived from FPN-AG at 460/505 nm was measured by fluorescence plate reader (Tecan Trading AG).

Sandwich ELISA

Regarding matching of antihepcidin mAbs, the sandwich ELISA pairs were first screened for suitability. The optimum concentrations of these pairs were selected by checkerboard titration. Next, sandwich ELISA was performed as follows: briefly, 96-well microtiter plates (Nalge Nunc International Corporation) were coated with antihepcidin mAbs against N-terminal sequence in a suitable concentration and incubated at room temperature for 1 h. After blocking with Blocking One (Nacalai Tesque, Inc.), synthetic hepcidin-25 in PBS/T was added and incubated for 2 h. Subsequently, wells were washed 4 times and incubated with biotinylated antihepcidin mAbs against 25 amino acids for 1 h. HRP-conjugated streptavidin was added and incubated for 1 h. Finally, after washing 4 times, each well was incubated with 100 µL TMB. The reaction was terminated by 25 µL 0.5N sulfuric acid, and the absorbance at 450 nm was read on a microplate reader, SoftMax Pro (Molecular Devices, LCC). For generation of a standard curve, 0.1-300 ng/mL of hepcidin-25 was used.

Preparation of samples to measure a variation in endogenous hepcidin levels

Lipopolysaccharide from *E. coli* O111: B4 (LPS; L2630, Sigma–Aldrich Co. LLC, St. Louis, MO) solution was diluted with saline for intravenous administration. For a single administration study, JTZ-951 (enarodustat; a hypoxia-inducible factor prolyl hydroxylase inhibitor) was chemically synthesized by Central Pharmaceutical Research Institute, Japan Tobacco, Inc. (Osaka,

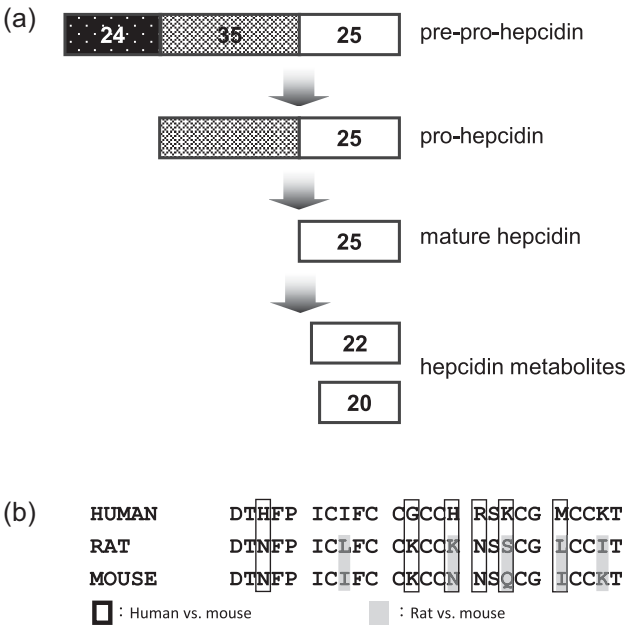

Figure 1. Posttranslational processing of hepcidin. Hepcidin is produced as a pre–proprotein with a typical N-terminal 24 amino acid endoplasmic reticulum-targeting signal sequence. (a) The signal peptide is removed when the proprotein enters the secretory pathway. Before secretion, the hepcidin is proteolytically cleaved between C-terminal of prodomain (35 amino acids) and N-terminal of hepcidin-25. At this time, hepcidin can form a hairpin structure stabilized by 4 disulfide bonds. Hepcidin-25 is further digested to smaller metabolites (22 and 20 amino acid). (b) Amino acid sequence alignment of human, rat, and mouse hepcidin is listed.

Japan). JTZ-951 was suspended in 0.5% (w/v) methyl cellulose solution for oral administration. The vehicle, JTZ-951, or LPS (Sigma–Aldrich Co. LLC) was administered to the rats. LPS at a dose of 1 mg/kg or JTZ-951 at a dose of 30 mg/kg was administered intravenously or perorally to 13-week-old male Sprague Dawley (SD) rats, respectively. Blood samples were collected from tail vein at the end of experimental period (8 h after each administration). Plasma from animals (4 conditions, $n = 2$) was prepared from venous blood obtained in heparin vacutainer vials (Becton, Dickinson and Company) by centrifugation at 1000 × g (10 min) followed by an additional centrifugation of collected plasma at 10 000 × g (10 min) to obtain low-platelet plasma. All samples were stored at −20°C until tested. For analysis by sandwich ELISA, samples were diluted with Assay Diluent (SurModics, Inc., Eden Prairie, MN) at room temperature followed by addition of BSA (0.6%), Triton X-100 (0.5%), and NaCl (274 mM).

Statistics

All data are expressed as mean ± standard deviation (SD). Statistical significance was determined by Williams multiple comparison test or Student's t-test. Differences were considered significant when P was less than 0.05.

Results and discussion

Generation of mAbs

Posttranslational processing of hepcidin was shown in Figure 1a. The basic properties of the mAbs generated against human, rat, and mouse hepcidin are listed in Table 1. Figure 2 shows the specificity of each mAbs against a sequence derived from

Table 1. The basic properties of the mAbs generated

Clone	Antigen source	Antigen	Isotype[a]
hHW1	Human	Whole hepcidin-25	IgG2b/k
hHW2	Human	Whole hepcidin-25	IgG2a/k
hHN1	Human	Hepcidin-25 N-term	IgG2b/k
rHN1	Rat	Hepcidin-25 N-term	IgG2b/k
rHN2	Rat	Hepcidin-25 N-term	IgG2b/k
rHN3	Rat	Hepcidin-25 N-term	IgG2a/k
mHW1	Mouse	Whole hepcidin-25	IgG2a/k

[a]Subclasses were determined with a mouse monoclonal antibody isotyping kit (GE Healthcare).

hepcidin. As shown in Figure 2a, we evaluated the reactivity against a peptide of N-terminal sequence of hepcidin-25 (a digested mature form) and a peptide including N-terminal sequence of hepcidin-25 following a sequence derived from prohepcidin (an undigested form). hHW1, hHW2, and mHW1 obtained from mice immunized with mature hepcidin-25 did not react against either a digested mature form or undigested form. On the other hand, hHN1, rHN1, and rHN2 obtained from mice immunized with N-terminal sequence reacted against only N-terminal edge sequence termed neo-epitope appearing after digestion by furin. Interestingly, rHN3 reacted against both a digested mature form and an undigested form. This means that mAb recognizes N-terminal sequence, not N-terminal edge. rHN1 had no cross-reactivity against peptide sequences of other species. As for human hepcidin, we evaluated the reactivity against hepcidin-25 biotinylated at aspartic acid of N-terminal edge (N-Bio-human hepcidin-25) and hepcidin-25 biotinylated at lysine of middle part (human hepcidin-25 K18-Bio). rHN1 reacted against human hepcidin-25 K18-Bio, in spite of showing no reaction against N-Bio-human hepcidin-25. In contrast, hHW1 and hHW2 reacted against both biotinylated forms (Figure 2b). It seems that these mAbs, except for rHN1, recognize middle part of mature hepcidin-25, not N-terminal edge. Next, we evaluated the reactivity against human hepcidin analogs. As hHW1 and hHW2 may recognize middle part of mature hepcidin-25, these mAbs seemed to react against all the human analogs (Figure 2c). However, these mAbs did not react against mouse hepcidin-25, as the alignment data on human versus mouse sequence seems to indicate that there are few potential epitopes (Figure 1). In Figure 2d, we evaluated the reactivity against prohepcidin (kindly gift from Y. Yamasaki) in sandwich mode. Briefly, anti-HAMP mAb (Abnova Corporation, Taipei City, Taiwan), which was obtained from mice immunized with a full length recombinant hepcidin (84 amino acids), was coated in a microtiter plate, and it captured prohepcidin. We subsequently tried detection using each mAb we generated. Although hHW1 and hHW2 detected prohepcidin depending on dilution rate, the combination with hHN1 did not detect prohepcidin, because hHN1 recognizes neo-epitope at N-terminal edge, and may react against mature hepcidin-25 only. As for rat/mouse, we evaluated the capability of antigen capture of mAbs. Monoclonal antibodies obtained from mice immunized with rat or mouse antigen did not capture human hepcidin-25 (Figure 2e and f).

Function of an expressed FPN-AG and activity of a synthetic hepcidin

To confirm a basic phenomenon, that is, that hepcidin may induce FPN internalization and degradation, we first established T-REx 293 cell line expressing human FPN with a C-terminal

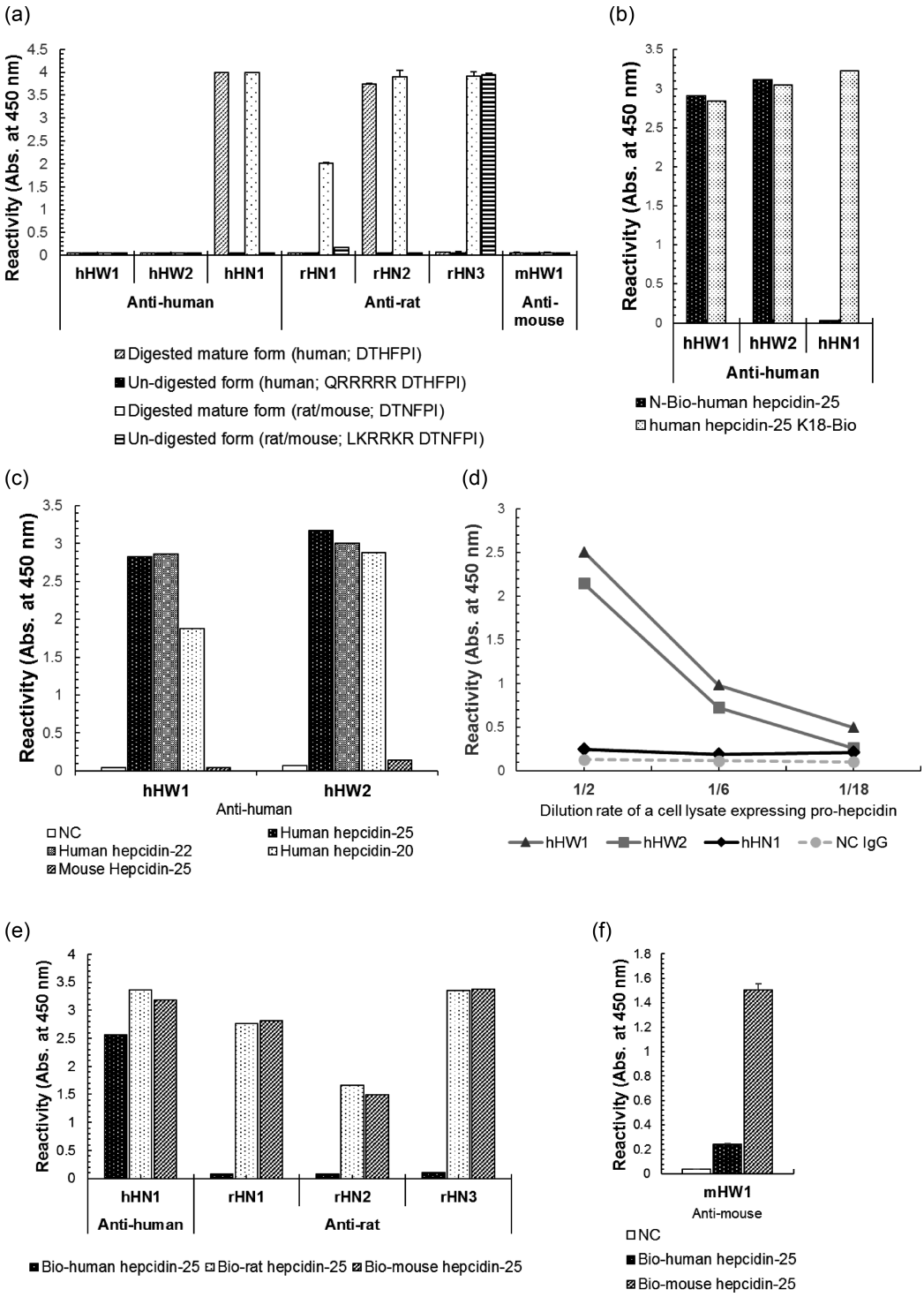

Figure 2. Reactivity of individual mAbs with hepcidin analyzed by ELISA. (a) Peptides derived from hepcidin linked to a C-terminal biotin-tag were incubated in streptavidin-coated wells and subsequently detected with each mAb. (b) N-Bio-human hepcidin-25 and human hepcidin-25 K18-Bio were incubated in streptavidin coated wells and subsequently detected with each mAb. (c) The hepcidin analogs were directly coated in wells of microtiter plate and subsequently were detected by each mAb. (d) Prohepcidin captured by anti-HAMP mAb (Abnova Corporation) was detected with each mAbs in sandwich mode. (e) Monoclonal antibodies were captured in protein G–coated wells and then biotinylated-human, biotinylated-rat, and biotinylated-mouse hepcidin-25 were incubated, and subsequently detected with streptavidin-HRP. (f) Monoclonal antibody was captured in protein G–coated wells and then biotinylated-human and biotinylated-mouse hepcidin-25 were incubated, and subsequently detected with streptavidin-HRP. The clone ID of each mAb is given on the X-axis and the absorbance at 450 nm on the Y-axis.

green fluorescent protein, AG (MBL Co.), under the control of the Tet-inducible CMV promoter. As a result, the quantity of FPN-AG estimated in terms of FIU at 460/505 nm increased in a dose-dependent manner, and the addition of over 0.1 μg/mL Tet seemed sufficient to induce FPN expression compared with negative control (Figure 3a). Expression of FPN-AG visualized with cellular imaging was ascertained on a cell surface (eg in Figure 3b left). Next, responsiveness to synthetic hepcidin-25 on FPN-AG internalization and degradation was evaluated. Cells expressing FPN-AG induced by 0.1 μg/mL Tet treatment for 24 h were incubated for 8 h in the presence or absence of 2 μg/mL human hepcidin-25, and then FIU at 460/505 nm was measured. FPN-AG that had increased clearly by the addition of Tet was obviously decreased by the addition of hepcidin-25 (Figure 3a). The quantity of FPN-AG estimated by western blot analysis with densitometry was also obviously decreased (data not shown), and this decrease of FPN-AG protein was inhibited by the addition of lysosome inhibitor chloroquine, but not proteasome inhibitor epoxomicin (data not shown). This means that FPN-AG was degraded by lysosome dependently through endocytosis. On the other hand, FPN-AG was ubiquitinated at 30 min after the addition of hepcidin-25 (data not shown). It seems that ubiquitination of FPN-AG functioned as a trigger of endocytosis start. When we evaluated FPN-AG degradation with several hepcidin-resistant mutants, C326Y was not ubiquitinated in spite of the addition of hepcidin-25, and remained on cell surface (data not shown). Figure 3b shows FPN-AG internalization visualized with cellular imaging using confocal microscopy. Cell surface expression of FPN-AG obviously disappeared at 5 h after the addition of hepcidin-25. Regarding the synthetic hepcidin-25, we also checked its activity against 3 other hepcidin-25 products purchased from sources other than the Peptide Institute, Inc. Only the hepcidin-25 obtained from Peptide Institute, Inc. had an activity capable of internalization of FPN-AG (data not shown). As hepcidin-25 is a tightly folded polypeptide with a hairpin structure stabilized by 4 disulfide bonds (Hunter *et al.* 2002), we supposed that the 3 other hepcidin-25 products did not have the proper conformational structure. Thus, we entrusted synthesis of all of hepcidin analogs for subsequent experiments to Peptide Institute, Inc.

Moreover, function of FPN-AG as an iron transporter was validated by ferritin accumulation assay. The T-REx 293 FPN-AG cells were incubated with 10 μM FAC in the presence or absence of 0.1 μg/mL Tet for 24 h. Cells were harvested, and ferritin content was determined by ELISA. FAC addition resulted in increased ferritin in cells. Ferritin accumulation that was prevented by the simultaneous addition of Tet was recovered by the addition of hepcidin-25 in a dose-dependent manner (Figure 3c).

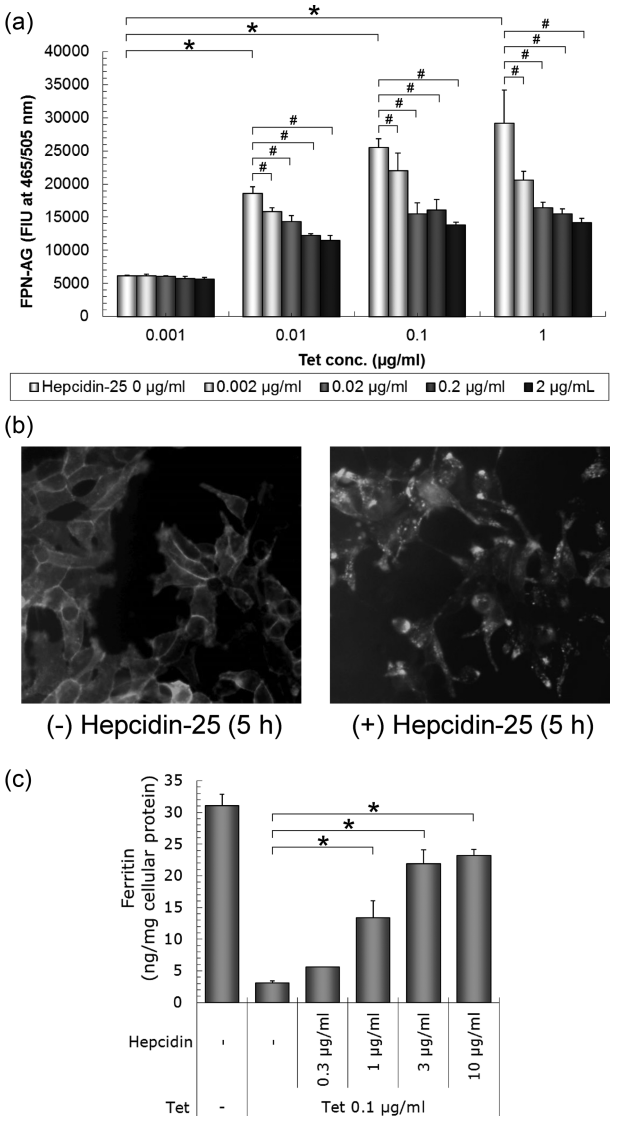

Figure 3. Expression of a functional FPN-AG on cell surface. T-REx 293 cells were stably transfected with a plasmid containing a Tet-regulated human FPN-AG construct. (a) FPN-AG was induced by 0.1 μg/mL Tet treatment for 24 h. Cells were then incubated for 9 h in the presence or absence of 2 μg/mL human hepcidin-25 and FIU at 460/505 nm was measured by fluorescence plate reader (Tecan Trading AG). FPN-AG induced by the addition of Tet was decreased by the addition of hepcidin-25. Bar represents the mean ± SD. Differences between the control (0.001 μg/mL Tet) without hepcidin treatment and 0.01-1 μg/mL Tet-treated cells without hepcidin treatment were determined by Williams multiple comparison test, and are considered significant at $P < 0.025$, as denoted by the asterisk. Differences between the control (0 μg/mL hepcidin-25) and 0.02-2 μg/mL hepcidin-25-treated cells were also determined by Williams multiple comparison test, and are considered significant at $P < 0.025$, as denoted by the hash mark. (b) FPN-AG was induced by 0.1 μg/mL Tet treatment for 24 h. Cells were then incubated for 5 h in the presence or absence of 2 μg/mL human hepcidin-25 and imaged by fluorescence microscopy. Bioactive hepcidin-25 induced the internalization of FPN-AG. (c) The resulting T-REx 293 FPN-AG cells were incubated with 10 μM FAC in the presence or absence of 0.1 μg/mL Tet for 24 h. Cells were harvested, and ferritin content was determined by ELISA. FAC addition resulted in increased ferritin in cells. Ferritin accumulation that was prevented by the simultaneous addition of Tet was recovered by the addition of hepcidin-25 in a dose-dependent manner. Bar represents the mean ± S.D. Differences between the control (0.1 μg/mL Tet without hepcidin-25) and 0.1 μg/mL Tet with 0.3-10 μg/mL hepcidin-25-treated cells were determined by Williams multiple comparison test, and are considered significant at $P < 0.025$, as denoted by the asterisk.

Effect of hepcidin analogs on FPN degradation

T-REx 293 FPN-AG cells were incubated with of 0.1 μg/mL Tet for 24 h. The cells were washed and then incubated at 37 °C at varying concentrations of human hepcidin-25, hepcidin-22, and hepcidin-20 (0.01-3 μg/mL) for 5 h. Figure 4a shows that human hepcidin-25, but not hepcidin-22 or hepcidin-20, induced degradation of FPN-AG. Importance of N-terminal amino acids for human hepcidin function (Hintze and McClung 2011; Andrade-Oliveira *et al.* 2015) was also demonstrated in our assay system. Next, we determined the function of rodent hepcidin-25. T-REx 293 expressing FPN-AG were incubated at varying concentrations of rat and mouse hepcidin-25. As a result, Figure 4b demonstrates that rat and mouse hepcidin-25 had the same activity on FPN-AG degradation compared with

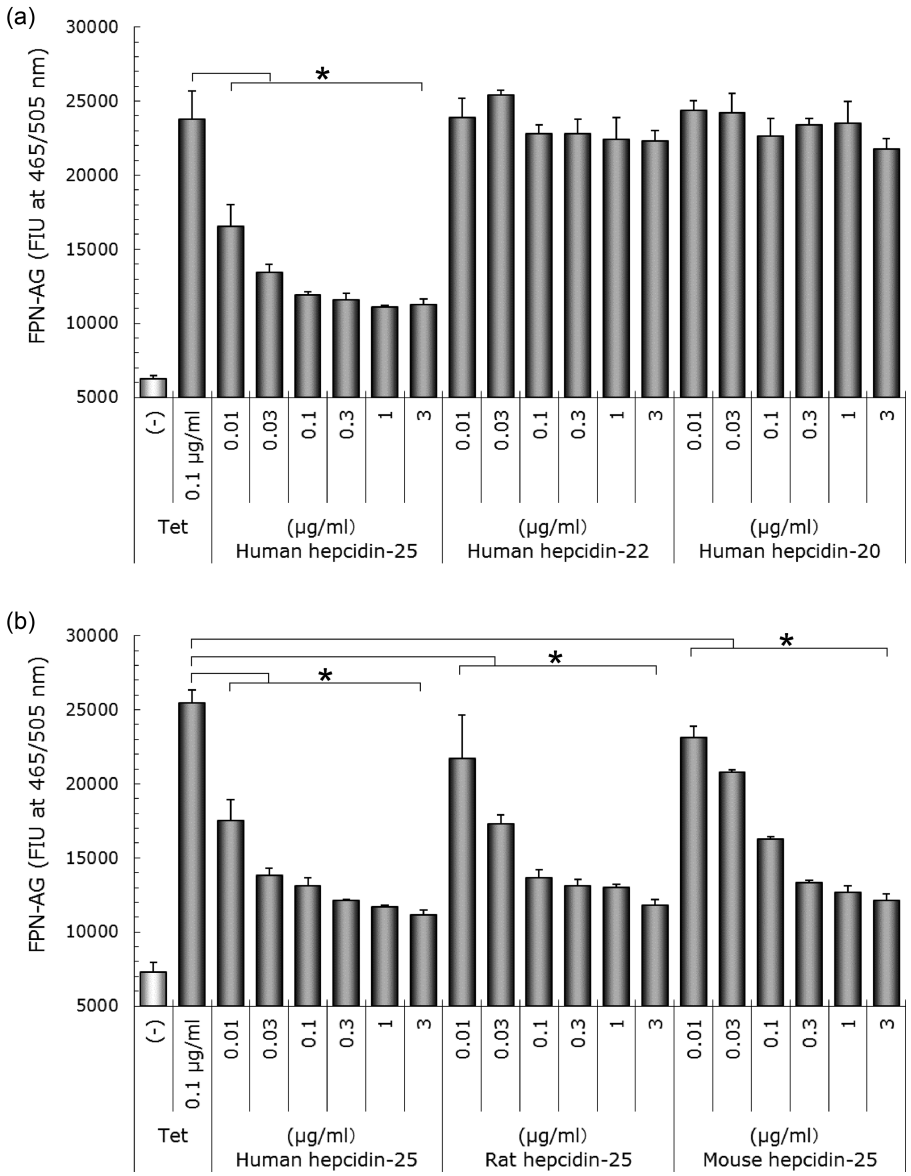

Figure 4. Effect of hepcidin analogs or its species on decrease of FPN-AG. (a) FPN-AG was induced by 0.1 μg/mL Tet treatment for 24 h. Cells were then incubated for 8 h in the presence or absence of 0.01-0.3 μg/mL human hepcidin-25, hepcidin-22, hepcidin-20, and FIU (460/505 nm) was measured. FPN-AG induced by Tet was decreased only by the addition of hepcidin-25, and not by hepcidin-22 or hepcidin-20. (b) Rat hepcidin-25 decreased the FPN-AG quantity induced by the addition of Tet in similar dose-dependent manner as with human hepcidin-25. Bar represents the mean ± SD. Differences between the control (0.1 μg/mL Tet without hepcidin-25) and 0.1 μg/mL Tet with hepcidin-25-treated cells were determined by Williams multiple comparison test, and are considered significant at $P < 0.025$, as denoted by the asterisk.

human hepcidin-25 as a positive control, in a dose-dependent manner. Therefore, we used synthetic hepcidin-25 of each species for subsequent experiments.

Neutralization of FPN-AG degradation by antihepcidin mAbs

Neutralization activity of antihepcidin mAbs on hepcidin-induced FPN-AG degradation was evaluated. The results are shown in Figure 5. Prior to addition of hepcidin-25, each mAb was incubated with hepcidin-25 for 1 h. Neutralization activity was estimated by FIU derived from FPN-AG at 6 h after the addition of mAbs–hepcidin-25 mixture. In the condition without hepcidin-25 addition, each mAb had no effect on the expression of FPN-AG induced by Tet. At least 2 clones of antihuman hepcidin-25 we checked protected FPN-AG from hepcidin-induced degradation in a dose-dependent manner (Figure 5). Additionally, in preliminary experiments, some clones of antirat hepcidin-25 protected FPN-AG from hepcidin-induced degradation (data not shown). At the view point of hepcidin-neutralizing activity, there was no remarkable difference between mAbs recognizing N-terminal edge and mAbs recognizing middle part of hepcidin-25. This might be thought that as hepcidin-25 is quite small compared with the size of immunoglobulin, the strength of neutralizing activity depends on an affinity against antigen prefer than a recognition site. Regarding hepcidin-neutralizing mAbs, a fully humanized mAb with high affinity was already developed and its capacity for iron mobilization in anemia patients was reported in a phase 1 study (Vadhan-Raj *et al.* 2017). It seems that these neutralizing mAbs may be useful tools for study on hepcidin–ferroportin axis among various diseases following

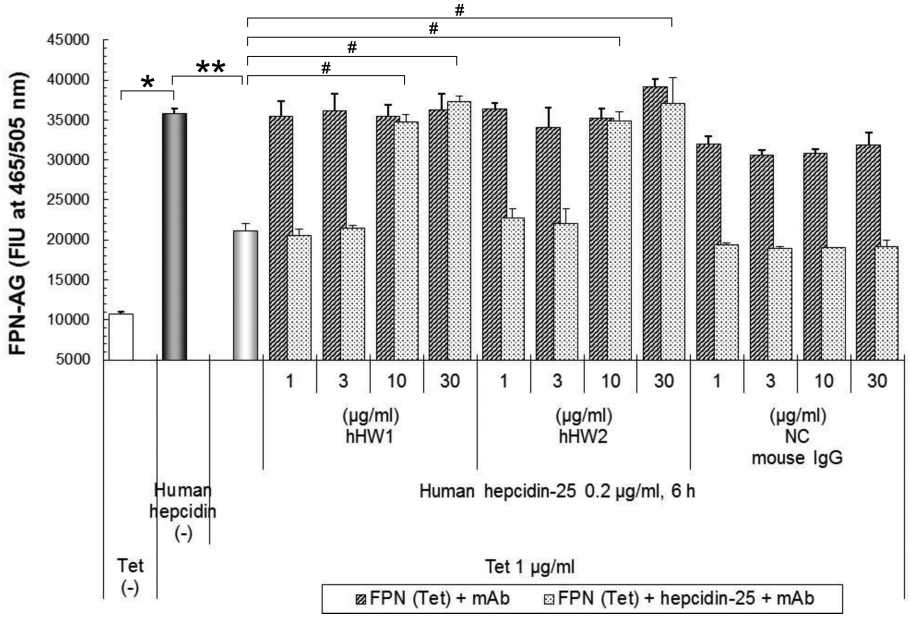

Figure 5. Neutralization activity of antihepcidin mAbs against hepcidin-induced FPN-AG degradation. FPN-AG was induced by 0.1 μg/mL Tet treatment for 24 h. Prior to addition of hepcidin-25, each mAb was incubated with hepcidin-25 for 30 min. Cells were then incubated in the presence of mAbs-hepcidin-25 mixture for 6 h. Antihuman hepcidin-25 mAbs were protective against hepcidin-induced FPN-AG degradation in a dose-dependent manner. Bar represents the mean ± SD. Differences between the control (no treatment) and 1 μg/mL Tet-treated cells were determined by Student's *t*-test, and are considered significant at $P < 0.000001$, as denoted by the asterisk. Differences between 1 μg/mL Tet-treated cells and 1 μg/mL Tet with 0.2 μg/mL hepcidin-25-treated cells were also determined by Student's *t*-test, and are considered significant at $P < 0.00005$, as denoted by the double asterisk. Differences between the control (1 μg/mL Tet with 0.2 μg/mL hepcidin-25-treated cells without mAb) and mAb-treated cells were determined by Williams multiple comparison test, and are considered significant at $P < 0.025$, as denoted by the hash mark.

decrease of iron availability in both *in vitro* cell systems and *in vivo* models. In addition, inhibition of hepcidin–ferroportin pathway by a small molecule that is able to antagonize ferroportin–hepcidin interaction was also reported (Ross *et al*. 2017). The authors identified an FPN antagonist that target is ferroportin, not hepcidin, capable of maintaining FPN iron export in the presence of elevated hepcidin concentrations, as occurs in chronic inflammatory conditions. Although there is currently little evidence as to which is the better way and proper target to ameliorate iron-related diseases, a plenitude of these useful tools may advance the understanding of the FPN–hepcidin interaction and thereby contribute to establishment of a strategy to define efficacy criteria as single agents in humans in the near future.

Sandwich ELISA development

These generated mAbs were further characterized for use in the quantitative determination based on sandwich mode, that is, the mAb conjugated with HRP used in the sandwich ELISA for detection of captured hepcidin. In general, sandwich mode is thought to be a quite sensitive and highly specific test system when compared with common and commercial competitive ELISA. Based on the results of experiments characterizing mAbs (Figure 2), we evaluated combinations of all mAbs. The evaluation was conducted in 2 steps: we first screened its recognition capability against N-terminal edge of hepcidin-25 in capture ELISA with each hepcidin-25 biotinylated at lysine of middle part, and then screened its detection capability in indirect ELISA with each mature hepcidin-25 biotinylated at aspartic acid of N-terminal edge.

The sandwich ELISA that was developed using clone hHN1 as capture antibody and biotinylated clone hHW1 as a detection reagent, successfully detected human hepcidin-25 in a dose-dependent manner. Regarding calibration, in the previous paper, the complexity of the problem on hepcidin measurement was revealed. A relative comparison of the assigned value of synthetic hepcidin-25 concentration from 2 vendors was performed, showing a difference of about 20% (Laarakkers *et al*. 2013). Therefore, we used an active form hepcidin-25, which was confirmed its activity by cell-based assay we established, as a calibrator. The standard curve using synthetic hepcidin-25 indicated that measurable amount of this assay was 0.1-100 ng/mL for human hepcidin-25 (a representative experiment is shown in Figure 6a). This combination did not react to prohepcidin, because there was no reactivity of capture mAb hHN1, and additionally had no detection signal against rat or mouse hepcidin-25, because there was no reactivity of detection mAb hHW1 against captured antigen (data not shown). The reason seemed to be due to steric hindrance between antigen and each mAbs in this mode.

Recently, the implication of hepcidin–ferroportin axis to pathogenesis and progression of diseases is focused not only on iron disorders such as anemia and kidney injury associated with CKD but also on metabolic disorders such as obesity and diabetes. To meaningfully interpret changes in serum or plasma hepcidin levels, it is thought to be essential to obtain adequate data on the variability of mature hepcidin, not total hepcidin levels in patients.

Measurement of hepcidin-25 in rat plasma

As for rat hepcidin-25, clone rHN1 together with mHW1-biotin yielded the best detection of hepcidin-25, allowing for the detection of 1-100 ng/mL of hepcidin-25. This combination also had no reactivity against human hepcidin-25 (Figure 6b). This combination (clone rHN1 and mHW1) also yielded the best detection of mouse hepcidin-25, allowing for the detection of 1-100 ng/mL of hepcidin-25. Unfortunately, this combination

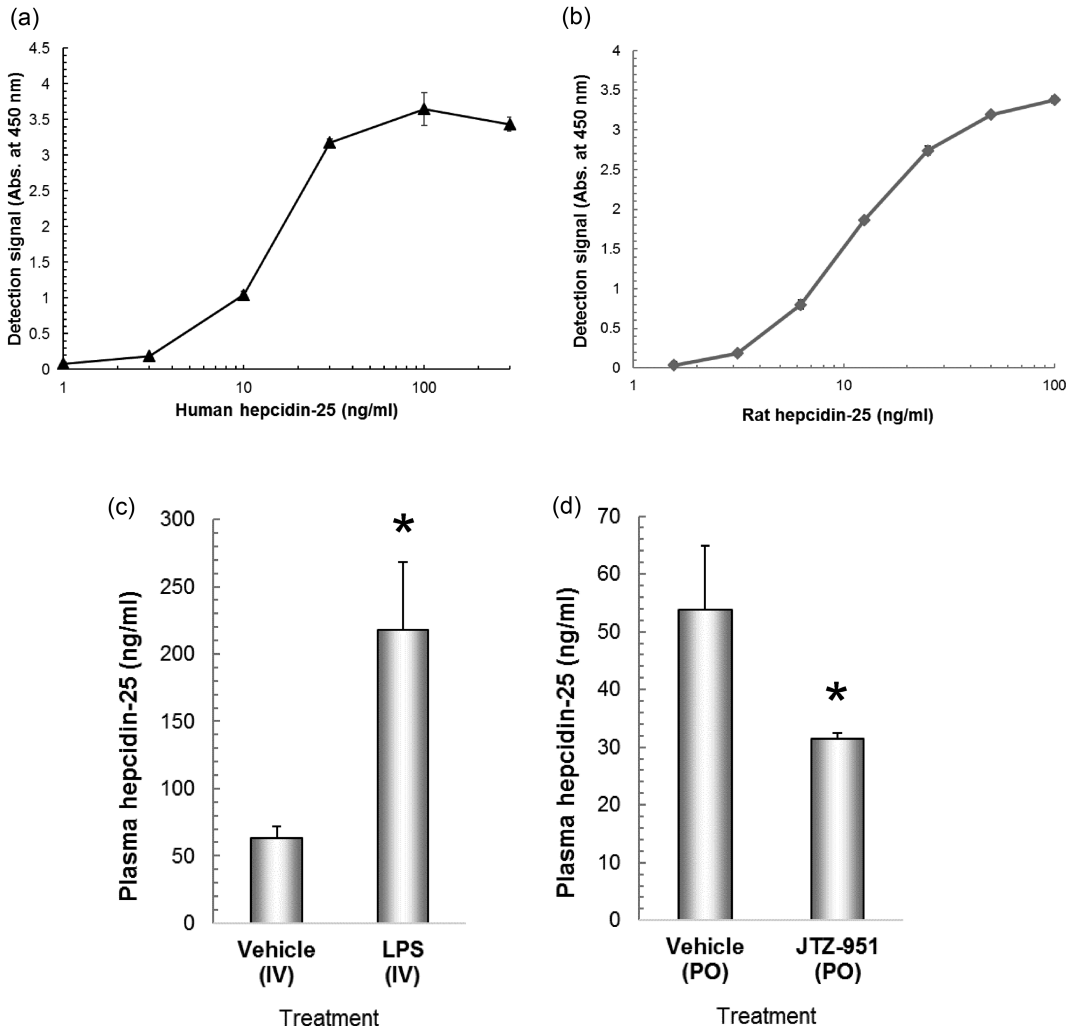

Figure 6. Variation analysis of hepcidin level in rat plasma using the sandwich ELISA. (a) A typical hepcidin-25 standard curve in the sandwich ELISA assay for human hepcidin-25. The values are mean absorbance counts at 450 nm ± SD ($n = 3$) from a single representative experiment. All experiments were performed at least twice. (b) A representative standard curve for synthetic rat hepcidin-25 is shown. (c) Overexpression of hepcidin in rat challenged with inflammatory stimulus. LPS at a dose of 1 mg/kg was administered intravenously (IV). Hepcidin in normal rat or in rat with LPS. (d) Effects on plasma hepcidin levels in rat after single administration of JTZ-951 ($n = 2$). JTZ-951 at a dose of 30 mg/kg was administered perorally (PO), and then hepcidin was measured at 8 h after administration. Bar represents the mean ± SD. Differences between the vehicle (control) and treated rats were determined by Student's *t*-test, and are considered significant at $P < 0.05$, as denoted by the asterisk.

had no reactivity against human hepcidin-25, because there was no cross reactivity of capture mAb rHN1 (Figure 2e).

To demonstrate the ability of this antibody to recognize the hepcidin in rodent samples, we used a rat biological model known to express hepcidin at mRNA level. Thus, rat hepcidin ELISA was performed on plasma samples from SD rat stimulated and nonstimulated with LPS and SD rat treated and untreated with JTZ-951, enarodustat. Prior to measurement of rodent samples, rat hepcidin ELISA was validated with respect to parallelism, recovery, and intra- and interassay variation (data not shown). As expected, the ELISA detected rat hepcidin-25 in SD rat plasma samples ($n = 2$ per conditions). When rat was challenged with LPS via i.v., the expressional level of hepcidin was obviously upregulated to 218.23 ng/mL. This was approximately 3 times the median levels of 63.00 ng/mL in samples not stimulated with LPS. On the other hand, the ELISA yielded median hepcidin levels of 53.75 ng/mL in samples not administered JTZ-951 via p.o. As JTZ-951 is a hypoxia-inducible factor prolyl hydroxylase (HIF-PH) inhibitor, and HIF-PH inhibitor is known to reduce serum hepcidin levels and is expected to provide the potential for correcting anemia with CKD by promoting endogenous EPO production (Ogoshi *et al.* 2017; Fukui *et al.* 2019), the expression level of hepcidin in samples administered with JTZ-951 was significantly downregulated to approximately half, 31.39 ng/mL (Figure 6c and d). As a proper alteration tendency of endogenous hepcidin level fluctuating with the treatment of inflammatory stimuli or suppressor was observed, it was demonstrated that this ELISA will enable examination of the variability of plasma hepcidin in various rodent models subjected to various stimuli.

Although hepcidin is thought to be a pleiotropic factor critical for many physiological and immunological conditions, there are few available research tools in general laboratories. For example, each mAb that are capable to discern immature, that is, pre–pro- and proform, and mature hepcidin-25 may be useful tool in the examination for the precise mechanism of pre–prohepcidin processing condition, not of gene expression change, in cells and tissues. Additionally, sufficient amount of mAbs usable in *in vivo*

animal studies that have a neutralizing activity against hepcidin may only be obtained individually through a special network except for own generating. These results may demonstrated that the use of the analytical tools we generated, that is, cell system, hepcidin derivatives, neutralizing mAbs, and measurable ELISA, may assist in excavating the potential role of hepcidin underlying various diseases, and also enable the assessment of a drug candidate's capacity to inhibit hepcidin–ferroportin axis in not only rodent models, but also human samples.

Conclusions

In this work, we developed several practical tools to study hepcidin and its receptor ferroportin axis.

- ✓ The generated T-REx 293 cell line expressing human FPN with a C-terminal green fluorescent protein under the control of the Tet-inducible promoter showed abundant fluorescence outlining the surface of cells within 24 h of Tet addition, leading to the accumulation of ferritin.
- ✓ Anti-hepcidin mouse mAbs that suppress ferroportin internalization by neutralizing hepcidin activity were generated.
- ✓ The developed Sandwich ELISA against hepcidin-25 is simple, reproducible, and ready for use in studies with rodent models and in clinical trials.

Acknowledgments

Many thanks to Dr. K. Fukui for generously providing *in vivo* rat samples and to Y. Yamasaki for kindly providing a cell lysate expressing prohepcidin. We are grateful to Dr. K. Suzuki for helpful discussions and expert advices.

Author contribution

S.S. conducted the establishment and verification of all of assays comprising FPN-AG internalization, ferritin accumulation, hepcidin activity neutralization, and sandwich ELISA in the course of this study, and also prepared this manuscript. M.K. and Y.M. generated antihepcidin mAbs and characterized their specificity in ELISA mode. Additionally, they also validated sensitivity and reproducibility in development of sandwich ELISA. Y.W. offered advice with dedication throughout this study.

Funding

None declared.

Disclosure statement

No potential conflict of interest was reported by the authors.

References

Abbas IM, Hoffmann H, Montes-Bayón M *et al.* Improved LC-MS/MS method for the quantification of hepcidin-25 in clinical samples. *Anal Bioanal Chem* 2018;**410**:3835-46.

Andrade-Oliveira V, Câmara NO, Moraes-Vieira PM. Adipokines as drug targets in diabetes and underlying disturbances. *J Diabetes Res* 2015;**2015**:681612.

Atanasiu V, Manolescu B, Stoian I. Hepcidin-central regulator of iron metabolism. *Eur J Haematol* 2007;**78**:1-10.

Barisani D, Pelucchi S, Mariani R *et al.* Hepcidin and iron-related gene expression in subjects with dysmetabolic hepatic iron overload. *J Hepatol* 2008;**49**:123-33.

Butterfield AM, Luan P, Witcher DR *et al.* A dual-monoclonal sandwich ELISA specific for hepcidin-25. *Clin Chem* 2010;**56**:1725-32.

Clark RJ, Tan CC, Preza GC *et al.* Understanding the structure/activity relationships of the iron regulatory peptide hepcidin. *Chem Biol* 2011;**18**:336-43.

Dahlfors G, Stål P, Hansson EC *et al.* Validation of a competitive ELISA assay for the quantification of human serum hepcidin. *Scand J Clin Lab Invest* 2015;**75**:652-8.

Fukui K, Shinozaki Y, Kobayashi H *et al.* JTZ-951 (enarodustat), a hypoxia-inducible factor prolyl hydroxylase inhibitor, stabilizes HIF-α protein and induces erythropoiesis without effects on the function of vascular endothelial growth factor. *Eur J Pharmacol* 2019;**859**:172532-8.

Gagliardo B, Kubat N, Faye A *et al.* Pro-hepcidin is unable to degrade the iron exporter ferroportin unless maturated by a furin-dependent process. *J Hepatol* 2009;**50**:394-401.

Ginzburg YZ. Hepcidin-ferroportin axis in health and disease. *Vitam Horm* 2019;**110**:17-45.

Girelli D, Nemeth E, Swinkels DW. Hepcidin in the diagnosis of iron disorders. *Blood* 2016;**127**:2809-13.

Hintze KJ, McClung JP. Hepcidin: a critical regulator of iron metabolism during hypoxia. *Adv Hematol* 2011;**2011**:510304.

Hunter HN, Fulton DB, Ganz T *et al.* The solution structure of human hepcidin, a peptide hormone with antimicrobial activity that is involved in iron uptake and hereditary hemochromatosis. *J Biol Chem* 2002;**277**:37597-603.

Teplan V Jr, F Vyhnánek, Gürlich R *et al.* Increased proinflammatory cytokine production in adipose tissue of obese patients with chronic kidney disease. *Wien Klin Wochenschr* 2010;**122**:466-73.

Konz T, Montes-Bayón M, Vaulont S. Hepcidin quantification: methods and utility in diagnosis. *Metallomics* 2014;**6**:1583-90.

Krause A, Neitz S, Mägert HJ *et al.* LEAP-1, a novel highly disulfide-bonded human peptide, exhibits antimicrobial activity. *FEBS Lett* 2000;**480**:147-50.

Kroot JJ, Tjalsma H, Fleming RE *et al.* Hepcidin in human iron disorders: diagnostic implications. *Clin Chem*. 201;**57**:1650-69.

Laarakkers CM, Wiegerinck ET, Klaver S *et al.* Improved mass spectrometry assay for plasma hepcidin: detection and characterization of a novel hepcidin isoform. *PLoS One* 2013;**8**:e75518.

Lefebvre T, Dessendier N, Houamel D *et al.* LC-MS/MS method for hepcidin-25 measurement in human and mouse serum: clinical and research implications in iron disorders. *Clin Chem Lab Med* 2015;**53**:1557-67.

Marmur J, Beshara S, Eggertsen G *et al.* Hepcidin levels correlate to liver iron content, but not steatohepatitis, in non-alcoholic fatty liver disease. *BMC Gastroenterol* 2018;**18**:78-87.

Nemeth E, Preza GC, Jung CL *et al.* The N-terminus of hepcidin is essential for its interaction with ferroportin: structure-function study. *Blood* 2006;**107**:328-33.

Nemeth E, Tuttle MS, Powelson J *et al.* Hepcidin regulates cellular iron efflux by binding to ferroportin and inducing its internalization. *Science* 2004;**306**:2090-3.

Ogoshi Y, Matsui T, Mitani I *et al.* Discovery of JTZ-951: a HIF prolyl hydroxylase inhibitor for the treatment of renal anemia. *ACS Med Chem Lett* 2017;**8**:1320-5.

Pandur E, Nagy J, Poór VS *et al.* Alpha-1 antitrypsin binds prepro-hepcidin intracellularly and prohepcidin in the serum. *FEBS J* 2009;**276**:2012-21.

Park CH, Valore EV, Waring AJ *et al*. Hepcidin, a urinary antimicrobial peptide synthesized in the liver. *J Biol Chem* 2001;**276**:7806-10.

Pihan-Le Bars F, Bonnet F, Loréal O *et al*. Indicators of iron status are correlated with adiponectin expression in adipose tissue of patients with morbid obesity. *Diabetes Metab* 2016;**42**:105-11.

Ross SL, Biswas K, Rottman J *et al*. Identification of antibody and small molecule antagonists of ferroportin-hepcidin interaction. *Front Pharmacol* 2017;**8**:838-58.

Sakamoto S, Tezuka K, Tsuji T *et al*. AILIM/ICOS: its expression and functional analysis with monoclonal antibodies. *Hybrid Hybridomics* 2001;**20**:293-303.

Senates E, Yilmaz Y, Colak Y *et al*. Serum levels of hepcidin in patients with biopsy-proven nonalcoholic fatty liver disease. *Metab Syndr Relat Disord* 2011;**9**:287-90.

Ueda N, Takasawa K. Role of hepcidin-25 in chronic kidney disease: anemia and beyond. *CMC* 2017;**24**:1417-52.

Vadhan-Raj S, Abonour R, Goldman JW *et al*. A first-in-human phase 1 study of a hepcidin monoclonal antibody, LY2787106, in cancer-associated anemia. *J Hematol Oncol* 2017;**10**:73-84.

Valore EV, Ganz T. Posttranslational processing of hepcidin in human hepatocytes is mediated by the prohormone convertase furin. *Blood Cells Mol Dis* 2008;**40**:132-8.

Wang CY, Babitt JL. Hepcidin regulation in the anemia of inflammation. *Curr Opin Hematol* 2016;**23**:189-97.